Q. J. R. Meteorol. Soc. (2007), **133**, pp. 1–21 doi: 10.1256/qj.yy.n

A regularization approach for a vertical slice model and semi-Lagrangian Störmer-Verlet time-stepping

By T. Hundertmark and S. Reich*
Universität Potsdam, Potsdam, Germany

(Received 27 September 2006; revised 25 April 2007)

Summary

In this paper, we provide a systematic derivation of regularized equations for a non-hydrostatic and compressible vertical slice model of the dry atmosphere. The derivation is based on an analysis of a semi-implicit discretization of the equations of motion and the regularized formulation by Dubal et al. (2006) is obtained as a special case. An implementation of the regularized equations, using the second-order, centred-in-time, two-time-level semi-Lagrangian Störmer-Verlet method of (Reich, 2006), is discussed and a series of numerical experiments is conducted.

Keywords: semi-implicit semi-Lagrangian regularization vertical slice Euler equations

1. Introduction

Atmospheric models contain motions on many different time scales. Often only the "slow" solution components are of interest and different strategies for an efficient computation of such solutions have been proposed. One possibility is to formulate (filtered) equations for the slow dynamics only (see, for example, Lynch (1989)). Another methodology, called initialization, keeps some or all fast modes in the model equations but prepares the initial data so that no "fast" waves are excited (Hinkelmann, 1951). This methodology requires the use of semi-implicit (SI) or split-step time-stepping methods as pioneered by Robert (1969); Kwizak & Robert (1971); Robert et al. (1972) and Marchuk (1974), respectively. In this paper, we will further develop an alternative approach called *regularization*. The basic idea is to derive a set of regularized equations of motion, which can be integrated by explicit time-stepping methods while, at the same time, leaving the "slow" solution components of the given model equations unaltered. While Staniforth et al. (2007) treated the shallow-water equations on an f-plane, we will focus in this paper on a vertical slice atmospheric model.

Regularized vertical slice Euler fluid equations of motion have been proposed and analyzed on a linear equation level by Dubal et al. (2006). The analysis is based on earlier work by Frank et al. (2005) and Wood et al. (2006) on regularized shallow-water equations and their link to SI and semi-implicit semi-Lagrangian (SISL) methods (see, e.g., (Robert, 1982; Tanguay et al., 1990; Temperton & Staniforth, 1987)).

In this paper, we provide a systematic derivation of regularized vertical slice models and their numerical implementation. Our approach is based on the methodology described by Reich et al. (2007), which links regularized formulations and SI time discretization schemes in a systematic manner.

More precisely, we consider a non-hydrostatic and compressible vertical slice model and its discretization by a simple SI method (without the semi-Lagrangian (SL) aspect). An appropriate reformulation, similar to Reich et al. (2007), suggests a regularized formulation, which can be discretized by a second-order, centred-in-time, two-time-level (2-TL), non-extrapolating time-stepping

* Corresponding author: Universität Potsdam, Institut für Mathematik, D-14469 Potsdam, Germany (e-mail: sreich@math.uni-potsdam.de)

method. In this paper, we discuss in particular the semi-Lagrangian Störmer-Verlet (SLSV) method of Reich (2006). The SLSV implementation requires the solution of a single elliptic problem per time step. See, for example, Bénard (2003) for a discussion of related 2-TL SISL schemes.

The new approach is validated by a series of numerical experiments.

2. Vertical slice Euler model

We consider a vertical slice model for a non-rotational atmosphere without orography. The Euler fluid equations of motion using a vertical height coordinate are given by

$$\frac{\partial u}{\partial t} = -\mathcal{A}(u) - c_p\theta\frac{\partial \pi}{\partial x}, \tag{1}$$

$$\frac{\partial w}{\partial t} = -\mathcal{A}(w) - c_p\theta\frac{\partial \pi}{\partial z} - g, \tag{2}$$

$$\frac{\partial \pi}{\partial t} = -\mathcal{A}(\pi) - \pi\frac{\kappa}{1-\kappa}\left(\frac{\partial u}{\partial x} + \frac{\partial w}{\partial z}\right), \tag{3}$$

$$\frac{\partial \theta}{\partial t} = -\mathcal{A}(\theta), \tag{4}$$

with parameter $\kappa \equiv R/c_p \approx 2/7$. Here u denotes the horizontal velocity, w the vertical velocity, π the Exner function, and θ potential temperature (Durran, 1998). Furthermore, $\mathcal{A}(X)$ denotes the advection operator of a quantity X, defined by

$$\mathcal{A}(X) \equiv \frac{DX}{Dt} - \frac{\partial X}{\partial t} = u\frac{\partial X}{\partial x} + w\frac{\partial X}{\partial z}. \tag{5}$$

The thermodynamic relation

$$\frac{R}{p_s}\rho\theta = \pi^{\frac{1-\kappa}{\kappa}} \tag{6}$$

between density, ρ, potential temperature, θ and Exner function, π, allows us to derive the following identities for frequent use throughout the paper:

$$\frac{\partial \pi}{\partial x} = \frac{\kappa}{1-\kappa}\frac{\pi}{\rho\theta}\frac{\partial(\rho\theta)}{\partial x} = \frac{c_s^2}{c_p\rho\theta^2}\frac{\partial(\rho\theta)}{\partial x}, \tag{7}$$

$$\frac{\partial \pi}{\partial z} = \frac{\kappa}{1-\kappa}\frac{\pi}{\rho\theta}\frac{\partial(\rho\theta)}{\partial z} = \frac{c_s^2}{c_p\rho\theta^2}\frac{\partial(\rho\theta)}{\partial z}, \tag{8}$$

where the speed of sound, c_s, is defined by

$$c_s^2 \equiv c_pT\frac{\kappa}{1-\kappa} = c_p\theta\pi\frac{\kappa}{1-\kappa} \tag{9}$$

and T denotes temperature. For example, it follows that (3) is equivalent to

$$\frac{\partial \pi}{\partial t} = -\frac{c_s^2}{c_p\rho\theta^2}\left[\frac{\partial}{\partial x}\{\rho\theta u\} + \frac{\partial}{\partial z}\{\rho\theta w\}\right]. \tag{10}$$

3. A SEMI-IMPLICIT DISCRETIZATION

We consider the following 2-TL SI method:

$$\frac{u^{n+1}-u^n}{\Delta t} = -\mathcal{A}(u^n) - c_p\theta^n\frac{\partial \pi^{n+1/2}}{\partial x}, \tag{11}$$

$$\frac{w^{n+1}-w^n}{\Delta t} = -\mathcal{A}(w^n) - c_p\left[\theta^n\frac{\partial \pi^{n+1/2}}{\partial z} + \theta^{n+1/2}\frac{\partial \pi^n}{\partial z} - \widehat{\theta}^{n+1/2}\frac{\partial \pi^n}{\partial z}\right] - g, \tag{12}$$

$$\frac{\pi^{n+1}-\pi^n}{\Delta t} = -\frac{(c_s^n)^2}{c_p\rho^n(\theta^n)^2}\left[\frac{\partial}{\partial x}\left\{\rho^n\theta^n u^{n+1/2}\right\} + \frac{\partial}{\partial z}\left\{\rho^n\theta^n w^{n+1/2}\right\}\right] \tag{13}$$

$$\frac{\theta^{n+1}-\theta^n}{\Delta t} = -u^n\frac{\partial \theta^n}{\partial x} - w^{n+1/2}\frac{\partial \theta^n}{\partial z}, \tag{14}$$

where we introduced the midpoint approximation of a quantity X by

$$X^{n+1/2} \equiv \frac{X^{n+1}+X^n}{2}, \tag{15}$$

the explicit midpoint predictor

$$\widehat{\theta}^{n+1/2} \equiv \theta^n - \frac{\Delta t}{2}\left(u^n\frac{\partial \theta^n}{\partial x} + w^n\frac{\partial \theta^n}{\partial z}\right), \tag{16}$$

and the density, ρ^n, by (6) using π^n and θ^n. The precise form of the numerical advection terms $\mathcal{A}(u^n)$ and $\mathcal{A}(w^n)$ is not relevant for the following discussion; one could apply Eulerian or SL approximations.

SISL discretizations such as the predictor-corrector formulation of the Unified Model (Davies et al., 2005) could also be considered. But such (more complex) discretization schemes would make the discussion rather technical. The particular formulation (11)-(14) has been chosen because it motivates the regularized equations of §4 in a rather natural manner.

The equations (11)-(14) can be implemented by first deriving the following set of linear equations in the midpoint values:

$$u^{n+1/2} = u^n - \frac{\Delta t}{2}\left[\mathcal{A}(u^n) + c_p\theta^n\frac{\partial \pi^{n+1/2}}{\partial x}\right], \tag{17}$$

$$w^{n+1/2} = w^n - \frac{\Delta t}{2}\left[\mathcal{A}(w^n) + c_p\theta^n\frac{\partial \pi^{n+1/2}}{\partial z} + c_p(\theta^{n+1/2} - \widehat{\theta}^{n+1/2})\frac{\partial \pi^n}{\partial z} + g\right], \tag{18}$$

$$\pi^{n+1/2} = \pi^n - \frac{\Delta t}{2}\frac{(c_s^n)^2}{c_p\rho^n(\theta^n)^2}\left[\frac{\partial}{\partial x}\left\{\rho^n\theta^n u^{n+1/2}\right\} + \frac{\partial}{\partial z}\left\{\rho^n\theta^n w^{n+1/2}\right\}\right], \tag{19}$$

$$\theta^{n+1/2} = \theta^n - \frac{\Delta t}{2}\left[u^n\frac{\partial \theta^n}{\partial x} + w^{n+1/2}\frac{\partial \theta^n}{\partial z}\right], \tag{20}$$

followed by an application of (15) to obtain the solutions at time-level t_{n+1}. We furthermore apply (20) and (16) to eliminate $\theta^{n+1/2}$ and $\widehat{\theta}^{n+1/2}$ from (18):

$$w^{n+1/2} = w^n - \frac{1}{1+\Delta t^2(\mathcal{N}^n)^2/4}\frac{\Delta t}{2}\left[\mathcal{A}(w^n) + c_p\theta^n\frac{\partial \pi^{n+1/2}}{\partial z} + g\right], \tag{21}$$

where

$$(\mathcal{N}^n)^2 \equiv -c_p \frac{\partial \pi^n}{\partial z}\frac{\partial \theta^n}{\partial z} \approx g\frac{\partial}{\partial z}\log\theta^n. \tag{22}$$

We now introduce a modification to (21). We note that the SI method (11)-(14) leads to a scaling of both advection and forcing terms in (21). A SL treatment (Staniforth & Coté, 1991) of advection would instead lead to a scaling of the vertical forcing terms only, which suggests to replace (21) by

$$w^{n+1/2} = w^n - \frac{\Delta t}{2}\mathcal{A}(w^n) + \frac{1}{1+\Delta t^2(\mathcal{N}^n)^2/4}\frac{\Delta t}{2}\left[c_p\theta^n\frac{\partial \pi^{n+1/2}}{\partial z} + g\right]. \tag{23}$$

A scaling of the vertical acceleration has also been suggested by Browning & Kreiss (1986). Their work is motivated by the bounded derivative principle and leads to a rather different factor of $(L_z/L_x)^2$, where L_z and L_x, respectively, are the vertical and horizontal, respectively, length scales.

The practical implementation of (17), (23), and (19)-(20) leads to a linearly implicit system in $\pi^{n+1/2}$. Similarly to the analysis provided by Reich et al. (2007) for a SI discretization of the shallow-water equations, we first introduce the midpoint predictor

$$\widehat{\pi}^{n+1/2} \equiv \pi^n - \frac{(c_s^n)^2}{c_p\rho^n(\theta^n)^2}\frac{\Delta t}{2}\left[\frac{\partial}{\partial x}\left\{\rho^n\theta^n u^n\right\} + \frac{\partial}{\partial z}\left\{\rho^n\theta^n w^n\right\}\right]. \tag{24}$$

This predictor corresponds to a forward Euler approximation to (10) over half a time-step. Next we substitute (17) and (23) into (19) and make use of (24) to obtain

$$\begin{aligned}\mathcal{H}^n\pi^{n+1/2} = \widehat{\pi}^{n+1/2} + \frac{(c_s^n)^2}{c_p\rho^n(\theta^n)^2}\frac{\Delta t^2}{4}\Bigg[&\frac{\partial}{\partial x}\left\{\rho^n\theta^n\mathcal{A}(u^n)\right\} \\ &+\frac{\partial}{\partial z}\left\{\rho^n\theta^n\left(\mathcal{A}(w^n) + \frac{g}{1+\Delta t^2(\mathcal{N}^n)^2/4}\right)\right\}\Bigg],\end{aligned} \tag{25}$$

with elliptic operator $\mathcal{H}^n$ defined by

$$\mathcal{H}^n f \equiv f - \frac{(c_s^n)^2}{\rho^n(\theta^n)^2}\frac{\Delta t^2}{4}\left[\frac{\partial}{\partial x}\left\{\rho^n(\theta^n)^2\frac{\partial f}{\partial x}\right\} + \frac{\partial}{\partial z}\left\{\frac{\rho^n(\theta^n)^2}{1+\Delta t^2(\mathcal{N}^n)^2/4}\frac{\partial f}{\partial z}\right\}\right]. \tag{26}$$

Provided the initial conditions are chosen appropriately (balanced initial conditions), we expect that $\widehat{\pi}^{n+1/2}$ is approximately equal to $\pi^{n+1/2}$ even for "large" step-sizes Δt. This observation is now developed further. In particular, we will derive a set of regularized fluid equations based on (25). The regularized fluid equations will reduce to the original Euler equations whenever

$$\widehat{\pi}^{n+1/2} \approx \pi^{n+1/2} \tag{27}$$

for the associated SISL discretization. Furthermore, we will demonstrate in §6 on a linearized equation level that fast unbalanced waves are slowed down for the regularized equations similar to what is achieved by the SISL method.

4. Regularized slice model

Following the work by Reich et al. (2007) on regularized shallow-water models and the regularized vertical slice formulation of Dubal et al. (2006), the analysis of §3 suggests to consider the following regularized form of the vertical slice model:

$$\frac{\partial u}{\partial t} = -\mathcal{A}(u) - c_p\theta\frac{\partial \tilde{\pi}}{\partial x}, \tag{28}$$

$$\frac{\partial w}{\partial t} = -\mathcal{A}(w) - \frac{1}{1+\alpha^2\mathcal{N}^2}\left[c_p\theta\frac{\partial \tilde{\pi}}{\partial z} + g\right], \tag{29}$$

$$\frac{\partial \pi}{\partial t} = -\frac{c_s^2}{c_p\rho\theta^2}\left[\frac{\partial}{\partial x}\left\{\rho\theta u\right\} + \frac{\partial}{\partial z}\left\{\rho\theta w\right\}\right], \tag{30}$$

$$\frac{\partial \theta}{\partial t} = -\mathcal{A}(\theta), \tag{31}$$

where

$$\mathcal{N}^2 \equiv g\frac{\partial}{\partial z}\log\theta. \tag{32}$$

The regularized Exner function, $\tilde{\pi}$, is determined by an elliptic problem of the general form

$$\mathcal{H}\left(\tilde{\pi} - \pi\right) = \alpha^2\mathcal{R}_\pi. \tag{33}$$

The elliptic operator, $\mathcal{H}$, and the RHS, $\alpha^2\mathcal{R}_\pi$, are chosen such that (33) mimics (25) under the identification $\tilde{\pi} \to \pi^{n+1/2}$ as well as $\pi \to \widehat{\pi}^{n+1/2}$ and discrete time-level t_n replaced by continuous time. More specifically, we define $\mathcal{R}_\pi$ by

$$\mathcal{R}_\pi \equiv \frac{c_s^2}{c_p\rho\theta^2}\left[\frac{\partial}{\partial x}\left(\rho\theta\mathcal{R}_u\right) + \frac{\partial}{\partial z}\left(\rho\theta\mathcal{R}_w\right)\right], \tag{34}$$

with

$$\mathcal{R}_u \equiv \mathcal{A}(u) + c_p\theta\frac{\partial \pi}{\partial x}, \qquad \mathcal{R}_w \equiv \mathcal{A}(w) + \frac{1}{1+\alpha^2\mathcal{N}^2}\left[c_p\theta\frac{\partial \pi}{\partial z} + g\right], \tag{35}$$

and the elliptic operator $\mathcal{H}$ by

$$\mathcal{H}f \equiv f - \frac{\alpha^2 c_s^2}{\rho\theta^2}\left[\frac{\partial}{\partial x}\left\{\rho\theta^2\frac{\partial f}{\partial x}\right\} + \frac{\partial}{\partial z}\left\{\frac{\rho\theta^2}{1+\alpha^2\mathcal{N}^2}\frac{\partial f}{\partial z}\right\}\right], \tag{36}$$

where $\alpha > 0$ is a free parameter, which will be determined in §6 based on a linear stability analysis.

The elliptic problem (33) can be transformed to

$$\mathcal{H}\tilde{\pi} = \pi + \frac{\alpha^2 c_s^2}{c_p\rho\theta^2}\left[\frac{\partial}{\partial x}\left\{\rho\theta\mathcal{A}(u)\right\} + \frac{\partial}{\partial z}\left\{\rho\theta\left(\mathcal{A}(w) + \frac{g}{1+\alpha^2\mathcal{N}^2}\right)\right\}\right], \tag{37}$$

and we note that, as desired, (37) with $\alpha = \Delta t/2$ is of the same form as (25).

Furthermore, we have $\tilde{\pi} = \pi$ whenever $\mathcal{R}_\pi = 0$. In that case $\mathcal{R}_u = -\partial u/\partial t$, $\mathcal{R}_w = -\partial w/\partial t$, and

$$c_p\theta^2\rho\mathcal{R}_\pi = -c_s^2\left\{\frac{\partial}{\partial x}\left(\theta\rho\frac{\partial u}{\partial t}\right) + \frac{\partial}{\partial z}\left(\theta\rho\frac{\partial w}{\partial t}\right)\right\} = 0. \tag{38}$$

Note that $\mathcal{R}_\pi = 0$ if, for example, $\partial\pi/\partial x = c_p\theta\partial\pi/\partial z + g = 0$ as well as $\mathcal{A}(u) = \mathcal{A}(w) = 0$ and, hence, a hydrostatic reference state leads to $\tilde{\pi} = \pi$. However, following (27), we only require the weaker condition $\tilde{\pi} \approx \pi$.

With a slight abuse of notation, we will call (37) a "nonlinear" regularization, while the corresponding form with the advection terms $\mathcal{A}(u)$ and $\mathcal{A}(w)$ set equal to zero will be called a "linear" regularization, i.e.

$$\mathcal{H}\tilde{\pi} = \pi + \frac{\alpha^2 c_s^2}{c_p\rho\theta^2}\frac{\partial}{\partial z}\left\{\frac{g\rho\theta}{1+\alpha^2\mathcal{N}^2}\right\}. \tag{39}$$

The elliptic problem (37) can be simplified by making use of additional assumptions such as that of a constant hydrostatic reference state. These simplifications are discussed in detail in the Appendix. Here we only summarize the formulations which will be implemented in the numerical experiments of §7. Given some hydrostatic reference state, characterized by $\bar{\pi}(z)$, $\bar{\theta}(z)$, $\bar{\rho}(z)$, and $\bar{c}_s(z)$, we introduce the constant coefficient elliptic operator

$$\mathcal{H}^F f \equiv f - \frac{\alpha^2\bar{c}_s^2}{\bar{\rho}\bar{\theta}^2}\left[\frac{\partial}{\partial x}\left\{\bar{\rho}\bar{\theta}^2\frac{\partial f}{\partial x}\right\} + \frac{\partial}{\partial z}\left\{\frac{\bar{\rho}\bar{\theta}^2}{1+\alpha^2\bar{\mathcal{N}}^2}\frac{\partial f}{\partial z}\right\}\right], \tag{40}$$

and replace (37) by

$$\mathcal{H}^F\tilde{\pi} = \pi + \frac{\alpha^2 c_s^2}{c_p\bar{\rho}\bar{\theta}^2}\left[\mathcal{W} + \frac{\partial}{\partial z}\left\{\frac{\bar{\rho}\bar{\theta}^2 g}{\theta(1+\alpha^2\bar{\mathcal{N}}^2)}\right\}\right] \tag{41}$$

with

$$\mathcal{W} \equiv \frac{\partial}{\partial x}\left\{\bar{\rho}\bar{\theta}\mathcal{A}(u)\right\} + \frac{\partial}{\partial z}\left\{\bar{\rho}\bar{\theta}\mathcal{A}(w)\right\}. \tag{42}$$

Note that $\mathcal{W}$ is set equal to zero in case of "linear" regularization. Note also that (50)-(41) with $\mathcal{W} = 0$ corresponds to the formulation proposed by Dubal et al. (2006).

We can simplify (41) even further under the assumption that

$$\frac{\mathrm{d}\bar{\pi}}{\mathrm{d}z} = 0, \qquad \frac{\mathrm{d}\bar{\theta}}{\mathrm{d}z} = 0, \qquad \bar{\mathcal{N}} = const., \qquad \bar{c}_s = const. \tag{43}$$

As shown in the Appendix, we obtain the system

$$\mathcal{H}^C\tilde{\pi} = \pi + \alpha^2\frac{\bar{c}_s^2}{c_p\bar{\theta}}\left[\frac{\partial}{\partial x}\left(\mathcal{A}(u)\right) + \frac{\partial}{\partial z}\left(\mathcal{A}(w)\right) + \frac{1}{1+\alpha^2\bar{\mathcal{N}}^2}\frac{\partial}{\partial z}\left(\frac{g\bar{\theta}}{\theta}\right)\right]. \tag{44}$$

with constant coefficient elliptic operator

$$\mathcal{H}^C f \equiv f - \alpha^2\left[\bar{c}_s^2\frac{\partial^2 f}{\partial x^2} + \frac{\bar{c}_s^2}{1+\alpha^2\bar{\mathcal{N}}^2}\frac{\partial^2 f}{\partial z^2}\right]. \tag{45}$$

Regularized formulations can also be derived in terms of pressure, p, and its regularization, $\tilde{p}$. The associated regularized Euler equations are stated in part (d) of the Appendix.

5. A description of the semi-Lagrangian Störmer-Verlet (SLSV) time discretization for the regularized vertical slice model

The temporal discretization of the regularized vertical slice model follows along the lines of the semi-Lagrangian Störmer-Verlet (SLSV) method proposed by Reich (2006). The SLSV method is based on the popular Störmer-Verlet time-stepping method for Newtonian dynamics of interacting particle systems (see, for example, Leimkuhler & Reich (2005)). Consider, for example, a single particle with position $q \in \mathbb{R}^3$, mass $m = 1$, velocity $u \in \mathbb{R}^3$, and applied force $F(q) \in \mathbb{R}^3$. The equations of motion are

$$\dot{q} = u, \qquad \dot{u} = F(q). \tag{46}$$

The Störmer-Verlet (SV) time-stepping reads now as follows:

Step 1 (half time step of velocity update):

$$u^{n+1/2} = u^n + \frac{\Delta t}{2} F(q^n). \tag{47}$$

Step 2 (full time step of force-free drift):

$$q^{n+1} = q^n + \Delta t u^{n+1/2}. \tag{48}$$

Step 3 (half time step of velocity update):

$$u^{n+1} = u^{n+1/2} + \frac{\Delta t}{2} F(q^{n+1}). \tag{49}$$

The two-time-level (2-TL) SV method is second-order, centred-in-time, and explicit. It also conserves linear and angular momentum in case of distant-dependent forces. See Leimkuhler & Reich (2005) for a detailed discussion.

For a continuum of particles (as in case of fluid dynamics), Step 2 is implemented in a semi-Lagrangian fashion to yield a grid-based method. This modification gives rise to the SLSV method of Reich (2006). We now describe the SLSV method in detail for the regularized vertical slice model with constant-coefficient regularization (41).

The SLSV method is based on the following reformulation of (28)-(31). We introduce material time derivatives $D(\cdot)/Dt = (\cdot)_t + \mathcal{A}(\cdot)$ and replace (30) by the mass continuity equation to obtain:

$$\frac{Du}{Dt} = -c_p \theta \frac{\partial \tilde{\pi}}{\partial x}, \tag{50}$$

$$\left[1 + \alpha^2 \bar{\mathcal{N}}^2\right] \frac{Dw}{Dt} = -c_p \theta \frac{\partial \tilde{\pi}}{\partial z} - g, \tag{51}$$

$$\frac{D \ln \rho}{Dt} = -\left(\frac{\partial u}{\partial x} + \frac{\partial w}{\partial z} \right), \tag{52}$$

$$\frac{D\theta}{Dt} = 0, \tag{53}$$

with π determined from ρ and θ by (6). The regularized Exner function $\tilde{\pi}$ is defined by (41). The implementation of the SLSV method consists now of three steps. (The spatial grid structure will be discussed in §7.)

Step 1 (half time step of Eulerian velocity update). Given the regularized Exner function $\tilde{\pi}^n$ we compute

$$u^{n+1/2-\varepsilon} = u^n - c_p\theta^n \frac{\Delta t}{2}\frac{\partial \tilde{\pi}^n}{\partial x}, \tag{54}$$

$$w^{n+1/2-\varepsilon} = w^n - \frac{1}{1+\alpha^2\bar{\mathcal{N}}^2}\frac{\Delta t}{2}\left[c_p\theta^n\frac{\partial \tilde{\pi}^n}{\partial z} + g\right]. \tag{55}$$

We use superscript $-\varepsilon$ in $(u^{n+1/2-\varepsilon}, w^{n+1/2-\varepsilon})$ to indicate that these are the grid values of (u, w) just before the advection step. Similarly, we will use superscript $+\varepsilon$ to denote the grid values of (u, w) immediately after the advection step which we describe next.

Step 2 (full time step of force-free advection). We first solve

$$\frac{Du}{Dt} = \frac{Dw}{Dt} = 0, \qquad \frac{Dx}{Dt} = u, \quad \frac{Dz}{Dt} = w \tag{56}$$

using a SL method (Staniforth & Coté, 1991; Durran, 1998). The exact solutions to (56) are given by linear trajectories, which we approximate using

$$x_a = x_d^n + \Delta t\, u_d^{n+1/2-\varepsilon}, \tag{57}$$

$$z_a = z_d^n + \Delta t\, w_d^{n+1/2-\varepsilon}, \tag{58}$$

where $(u_d^{n+1/2-\varepsilon}, w_d^{n+1/2-\varepsilon})$ are obtained from the grid values $(u^{n+1/2-\varepsilon}, w^{n+1/2-\varepsilon})$ by bilinear interpolation to the departure points. The arrival points (x_a, z_a) are identified with given grid points. The equations (57)-(58) are solved by applying two iterations of a simple fixed point algorithm (Smolarkiewicz & Pudykiewicz, 1992) and determine all departure points (x_d, z_d).

Once the departure point calculation has been completed, bicubic interpolation is used to first obtain $(u_d^{n+1/2-\varepsilon}, w_d^{n+1/2-\varepsilon})$ and, finally, the new updated values of $(u^{n+1/2+\varepsilon}, w^{n+1/2+\varepsilon})$ over the grid via

$$u^{n+1/2+\varepsilon} = u_d^{n+1/2-\varepsilon}, \qquad w^{n+1/2+\varepsilon} = w_d^{n+1/2-\varepsilon}. \tag{59}$$

We next advect the density ρ. We make use of formulation (52) and obtain the SL approximation

$$\left[\ln\rho^{n+1} + \frac{\Delta t}{2}\left(\frac{\partial u}{\partial x} + \frac{\partial w}{\partial z}\right)^{n+1/2+\varepsilon}\right]_a = \left[\ln\rho^{n} - \frac{\Delta t}{2}\left(\frac{\partial u}{\partial x} + \frac{\partial w}{\partial z}\right)^{n+1/2-\varepsilon}\right]_d, \tag{60}$$

where subscript a and d, respectively, denote arrival and departure point evaluation, respectively. The potential temperature θ is advected according to

$$\left[\theta^{n+1}\right]_a = \left[\theta^n\right]_d. \tag{61}$$

Bicubic interpolation is used for departure point approximations.

Step 3 (half time step of Eulerian velocity update). Given the Exner function π^{n+1}, potential temperature θ^{n+1}, and an approximation to $\mathcal{W}$ (see the following

remark), we first compute the regularized Exner function $\tilde{\pi}^{n+1}$ according to (41). The time step is completed by

$$u^{n+1} = u^{n+1/2+\varepsilon} - c_p \theta^{n+1} \frac{\Delta t}{2} \frac{\partial \tilde{\pi}^{n+1}}{\partial x}, \tag{62}$$

$$w^{n+1} = w^{n+1/2+\varepsilon} - \frac{1}{1+\alpha^2 \bar{\mathcal{N}}^2} \frac{\Delta t}{2} \left[c_p \theta^{n+1} \frac{\partial \tilde{\pi}^{n+1}}{\partial z} + g \right]. \tag{63}$$

Remark. In case of "nonlinear" regularization, expression (42) needs to be approximated. We make use of the procedure suggested by Reich et al. (2007) for the shallow-water equations, i.e.

$$\mathcal{W} \approx \left[\frac{\partial}{\partial x} \left\{ \bar{\rho} \bar{\theta} \frac{Du}{Dt} \right\} + \frac{\partial}{\partial z} \left\{ \bar{\rho} \bar{\theta} \frac{Dw}{Dt} \right\} \right] - \frac{D}{Dt} \left[\frac{\partial}{\partial x} \left\{ \bar{\rho} \bar{\theta} u \right\} + \frac{\partial}{\partial z} \left\{ \bar{\rho} \bar{\theta} w \right\} \right] \tag{64}$$

$$\approx 2 \left[\frac{\partial w}{\partial x} \frac{\partial}{\partial z} \left(\bar{\rho} \bar{\theta} u \right) - \frac{\partial u}{\partial x} \frac{\partial}{\partial z} \left(\bar{\rho} \bar{\theta} w \right) \right]. \tag{65}$$

Equation (64) can be approximated conveniently by the SL technique (Staniforth & Coté, 1991; Durran, 1998) using the arrival and departure points from *Step 2*, while (65) can be approximated directly using the current velocity values $(u^{n+1/2+\varepsilon}, w^{n+1/2+\varepsilon})$. Further details can be found in (Reich et al., 2007).

It can be shown that the 2-TL SLSV scheme given by (54)-(63) with $\mathcal{W} = 0$ is centered-in-time (up to higher order asymmetries due to interpolation and fixed point iteration errors in the semi-Lagrangian advection under *Step 2*). Hence the method is second-order in time for the regularized equations and "linear" balance. The case of "nonlinear" balance is more technical due to the necessary approximations to (64) or (65), respectively.

Note that the semi-Lagrangian advection in *Step 2* could be replaced by other methods suitable for advection problems (Durran, 1998). This applies, in particular, to the continuity equation (52) and we intend to replace (60) by the conservative remapped particle-mesh semi-Lagrangian method by Cotter et al. (2007) in future implementations.

6. A linear stability analysis

We now apply the regularization to a vertical slice model linearized about an isothermal stationary reference state with reference temperature T^*. Reference values are denoted by $\theta^* = \theta^*(z)$ etc. The resulting linear equations in the perturbative quantities (u', w', π', θ') are given by

$$\frac{\partial u'}{\partial t} = -c_p \theta^* \frac{\partial \pi'}{\partial x}, \tag{66}$$

$$\frac{\partial w'}{\partial t} = -c_p \theta^* \frac{\partial \pi'}{\partial z} + g \frac{\theta'}{\theta^*}, \tag{67}$$

$$\frac{\partial \pi'}{\partial t} = -w' \frac{\mathrm{d}\pi^*}{\mathrm{d}z} - \pi^* \frac{\kappa}{1-\kappa} \left(\frac{\partial u'}{\partial x} + \frac{\partial w'}{\partial z} \right), \tag{68}$$

$$\frac{\partial \theta'}{\partial t} = -w' \frac{\mathrm{d}\theta^*}{\mathrm{d}z}. \tag{69}$$

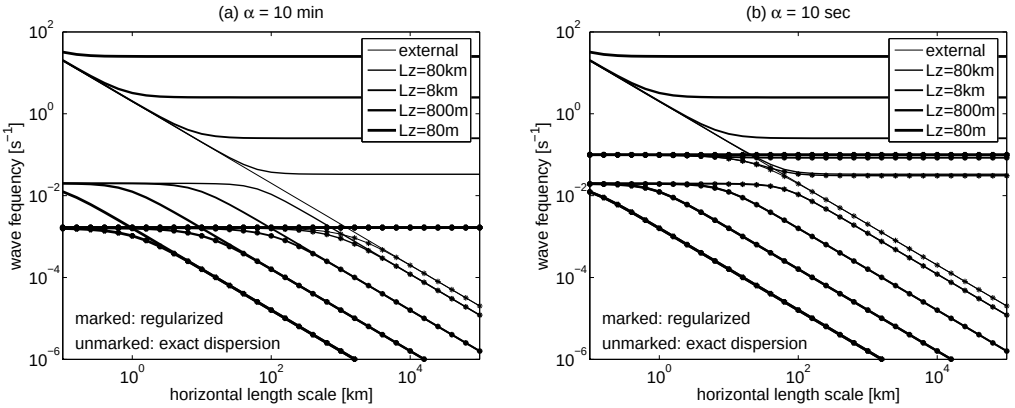

Figure 1. Dispersion relations for vertical slice model and its regularized formulation with the equations being linearized about a stationary isothermal reference state. The regularization parameter, α, is set equal to $\alpha = 10$ min in panel (a) and to $\alpha = 10$ s in panel (b), respectively. Lines corresponding to different vertical length scales, L_z, are plotted with increasing line width for decreasing L_z. For fixed L_z, each line represents wave frequency, ω, as a function of horizontal length scale, $L_x = 2\pi/k_x$.

The reference values satisfy

$$u^* = v^* = w^* = 0, \tag{70}$$

$$T^* = \text{constant}, \tag{71}$$

$$\theta^*(z) = T^* e^{\kappa z/H}, \tag{72}$$

$$\pi^*(z) = e^{-\kappa z/H}, \tag{73}$$

$$(c_s^*)^2 \equiv c_p T^* \tfrac{\kappa}{1-\kappa}, \quad (\mathcal{N}^*)^2 \equiv g\tfrac{d}{dz}\log\theta^*, \quad \Gamma^* \equiv \tfrac{1-2\kappa}{2H}, \quad H^* \equiv \tfrac{RT^*}{g}. \tag{74}$$

The associated regularized equations are

$$\frac{\partial u'}{\partial t} = -c_p\theta^*\frac{\partial \tilde{\pi}'}{\partial x}, \tag{75}$$

$$\frac{\partial w'}{\partial t} = \frac{-1}{1+\alpha^2(\mathcal{N}^*)^2}\left\{c_p\theta^*\frac{\partial \tilde{\pi}'}{\partial z} - g\frac{\theta'}{\theta^*}\right\}, \tag{76}$$

$$\frac{\partial \pi'}{\partial t} = -w'\frac{\mathrm{d}\pi^*}{\mathrm{d}z} - \pi^*\frac{\kappa}{1-\kappa}\left(\frac{\partial u'}{\partial x} + \frac{\partial w'}{\partial z}\right), \tag{77}$$

$$\frac{\partial \theta'}{\partial t} = -w'\frac{\mathrm{d}\theta^*}{\mathrm{d}z}, \tag{78}$$

with

$$\widehat{\mathcal{H}}\,\tilde{\pi}' = \pi' + \alpha^2(c_s^*)^2\left\{\frac{1}{1+\alpha^2(\mathcal{N}^*)^2}\frac{g}{c_p}\left[\frac{\partial}{\partial z} - 2\Gamma^*\right]\left(\frac{-\theta'}{(\theta^*)^2}\right)\right\} \tag{79}$$

and

$$\widehat{\mathcal{H}} f \equiv f - \alpha^2(c_s^*)^2\left[\frac{\partial^2 f}{\partial x^2} + \frac{1}{1+\alpha^2(\mathcal{N}^*)^2}\left(\frac{\partial^2 f}{\partial z^2} - 2\Gamma^*\frac{\partial f}{\partial z}\right)\right]. \tag{80}$$

The linearized equations and a time-staggered disretization have been analyzed by Dubal et al. (2006). In particular, we make the general *ansatz*:

$$X'(t,x,z) = \bar{X}(z)\exp(i\omega t)\ \exp(ik_x x). \tag{81}$$

A straightforward application of the results by Dubal et al. (2006)) reveals that all frequencies ω, present in the regularized system (75)-(79), are bounded by

$$\omega^2 \leqslant \frac{1}{\alpha^2}. \tag{82}$$

See Fig. 1 for a comparison of the exact and regularized dispersion relations for two different values of α.

On the other hand, the Störmer-Verlet time stepping method is linearly stable (see, e.g., Leimkuhler & Reich (2005)) for a harmonic oscillator with frequency ω provided the step-size Δt satisfies

$$\Delta t|\omega| \leqslant 2. \tag{83}$$

It follows that

$$\alpha \geqslant \frac{\Delta t}{2} \tag{84}$$

implies linear stability for the SLSV method of §5 applied to the regularized vertical slice model.

7. Numerical experiments

Experiments are performed with the SLSV method described in §5. The spatial discretization uses an Arakawa C-grid in the horizontal and a Charney-Phillips grid in the vertical with periodic boundary conditions in the horizontal and rigid boundary conditions $w = 0$ at $z = 0$ and $z = z_T$ (see, e.g., Durran (1998) for a discussion of these spatial discretization methods). The rigid boundary implies the boundary condition

$$\frac{\partial \tilde{\pi}}{\partial z} = 0 \quad \text{at} \quad z = 0, \;\; z = z_T \tag{85}$$

for the arising elliptic equation in $\tilde{\pi}$. The regularization parameter α is set equal to

$$\alpha = 1.1\frac{\Delta t}{2} \tag{86}$$

for all numerical experiments. A good indicator for the "strength" of the regularization is provided by the horizontal and vertical smoothing lengths defined by

$$l_x \equiv \bar{c}_s \alpha \tag{87}$$

and

$$l_z \equiv \frac{\bar{c}_s \alpha}{\sqrt{1 + \alpha^2 \bar{\mathcal{N}}^2}}, \tag{88}$$

respectively. If either $l_x \gg \Delta x$ and/or $l_z \gg \Delta z$, then the regularization has a strong filtering effect on non-balanced contributions to the Exner function π.

Results are compared to available reference solutions. See the *Standard Test Set* collected under `http://www.mmm.ucar.edu/projects/srnwp_tests` in particular.

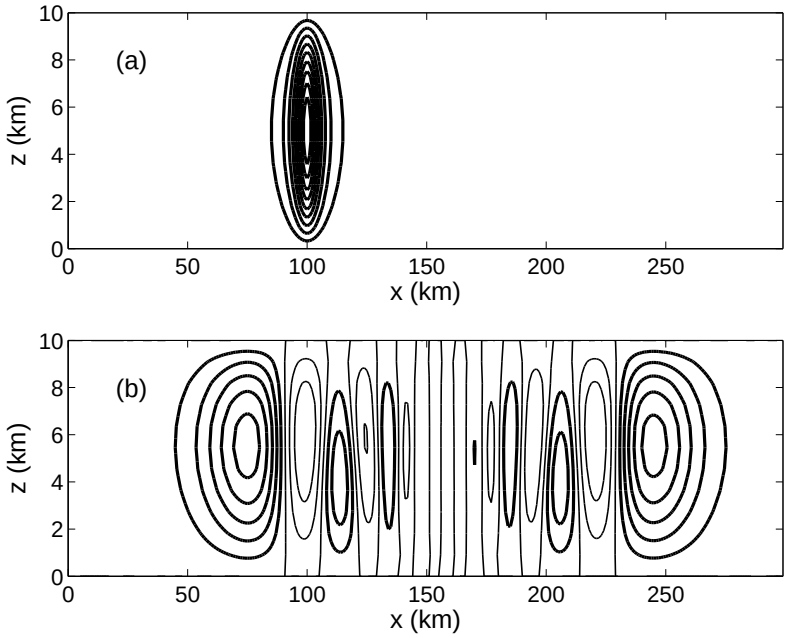

Figure 2. (a) Plots of θ' at initial time. (b) Plot of θ' at final time $t = 3000$ s. Computations are performed with the regularized SLSV method using a 500 m spatial grid resolution and a time-step of 12 s. The contour interval is 0.5×10^{-3} K. Thick lines indicate positive values of θ'.

(*a*) *Test case 1 from the Standard Test Set: Nonhydrostatic inertia gravity waves*

The reference solution and a detailed problem description can be found in Skamarock & Klemp (1994). However, in contrast to Skamarock & Klemp (1994), we computed the solution using the fully compressible vertical slice model with an isothermal hydrostatic reference state corresponding to $\bar{\mathcal{N}} = 0.01$ s^{-1} and $\bar{c}_s = 300$ m s^{-1}. We implemented the regularization from §5 with "linear" regularization, i.e., $\mathcal{W} = 0$ in (41).

The mesh-size is $\Delta x = \Delta z = 500$ m. The time-step is $\Delta t = 12$ s. This corresponds to a horizontal and vertical smoothing length of $l_x \approx l_z \approx 1800$ m. Note that $1 + (\Delta t \bar{\mathcal{N}}/2)^2 \approx 1$.

The results displayed in Fig. 2 are in excellent agreement with those of Skamarock & Klemp (1994) and even more so with those from the *Standard Test Set*.

(*b*) *Test case 1 from the Standard Test Set: Hydrostatic inertia gravity waves*

We now include the Coriolis term with $f = 10^{-4}$ s^{-1} and consider a channel of length $L_x = 6000$ km and height $L_z = 10$ km. The problem formulation is again as in (Skamarock & Klemp, 1994). However, in contrast to Skamarock & Klemp (1994), we computed the solution using the fully compressible vertical slice model

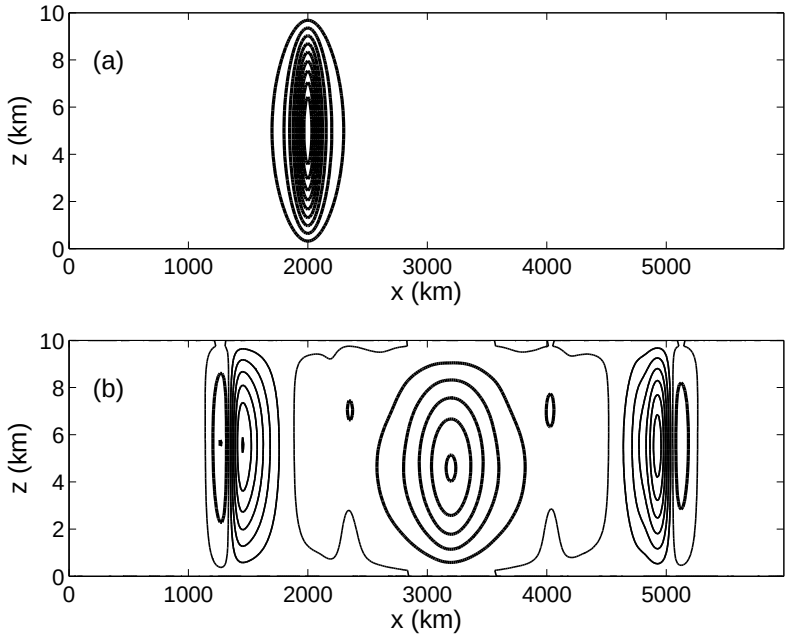

Figure 3. (a) Plot of θ' at initial time. (b) Plot of θ' at final time $t = 60,000$ s. Computations are performed with the regularized SLSV method using a 250 m vertical and a 20 km horizontal grid resolution. The time-step is $\Delta t = 200$ s. The contour interval is 0.5×10^{-3} K. Thick lines indicate positive values of θ'.

on an f-plane:

$$\frac{Du}{Dt} = fv - c_p\theta\frac{\partial\pi}{\partial x}, \tag{89}$$

$$\frac{Dv}{Dt} = -f(u - U_0), \tag{90}$$

$$\frac{Dw}{Dt} = -c_p\theta\frac{\partial\pi}{\partial z} - g, \tag{91}$$

$$\frac{D\rho}{Dt} = -\rho\left(\frac{\partial u}{\partial x} + \frac{\partial w}{\partial z}\right), \tag{92}$$

$$\frac{D\theta}{Dt} = 0, \tag{93}$$

where $U_0 = 20$ m s^{-1}. We implemented the regularization from §5 with "linear" regularization, i.e., $\mathcal{W} = 0$ in (41).

The mesh-size is $\Delta x = 20$ km and $\Delta z = 250$ m. The time-step is $\Delta t = 200$ s. This corresponds to a horizontal smoothing length of $l_x \approx 30$ km and a vertical smoothing length of $l_z \approx 21$ km, respectively.

The results displayed in Fig. 3 are again in excellent agreement with those of (Skamarock & Klemp, 1994) and with those provided in the *Standard Test Set*.

Remark. The effect of the Coriolis terms could be included in the regularization procedure as outlined by Wood et al. (2006). A detailed description will be the

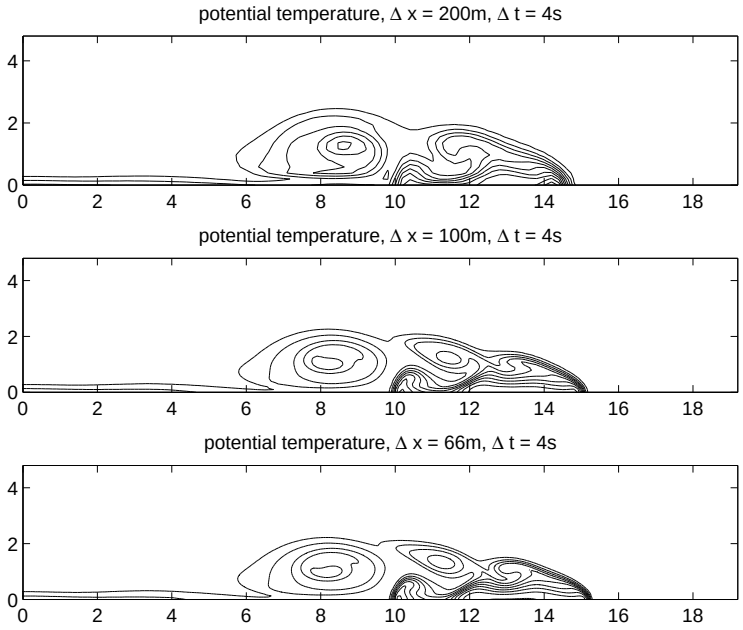

Figure 4. Plots of θ' at 900 s from the regularized SLSV method using (a) 200, (b) 100, and (c) 66 m spatial resolution and a time-step of 4 s. The minimum contour line is at $\theta' = -16.624$ K and the contour interval is 1 K.

subject of a forthcoming publication. For the current test problem such a more sophisticated regularization is not required.

(*c*) *Test case 2 from the Standard Test Set: Density current*

This test case has been very well documented by Straka et al. (1993). We implemented the regularized equations with a constant (reference) potential temperature $\bar{\theta} = 300$ K, a constant speed of sound $\bar{c}_s = 347$ m s^{-1}, $\bar{\mathcal{N}} = 0$, and with (44) further simplified to

$$\mathcal{H}^C \tilde{\pi} = \pi + \alpha^2 \frac{\bar{c}_s^2}{c_p} \frac{\partial}{\partial z} \left(\frac{g}{\theta} \right) \tag{94}$$

("linear" regularization). The results from Fig. 4 are in excellent agreement with the reference solutions provided in Straka et al. (1993). Even the simulation with a low resolution of $\Delta x = \Delta z = 200$ m yields a reasonable approximation. Note that $\Delta t = 4$ s corresponds to a vertical and horizontal smoothing length of $l_x \approx l_z \approx 694$ m.

(*d*) *Bubble convection test*

This test case has been proposed by Robert (1993). The motion of a larger warm bubble and a smaller cold bubble are considered in a neutrally stratified basic-state atmosphere of constant potential temperature $\theta = 30^o$ C. The bubbles are Gaussian shaped at initial time and well resolved over the computational grid with grid-size $\Delta x = \Delta z = 5$ m. Our setting corresponds exactly to that of

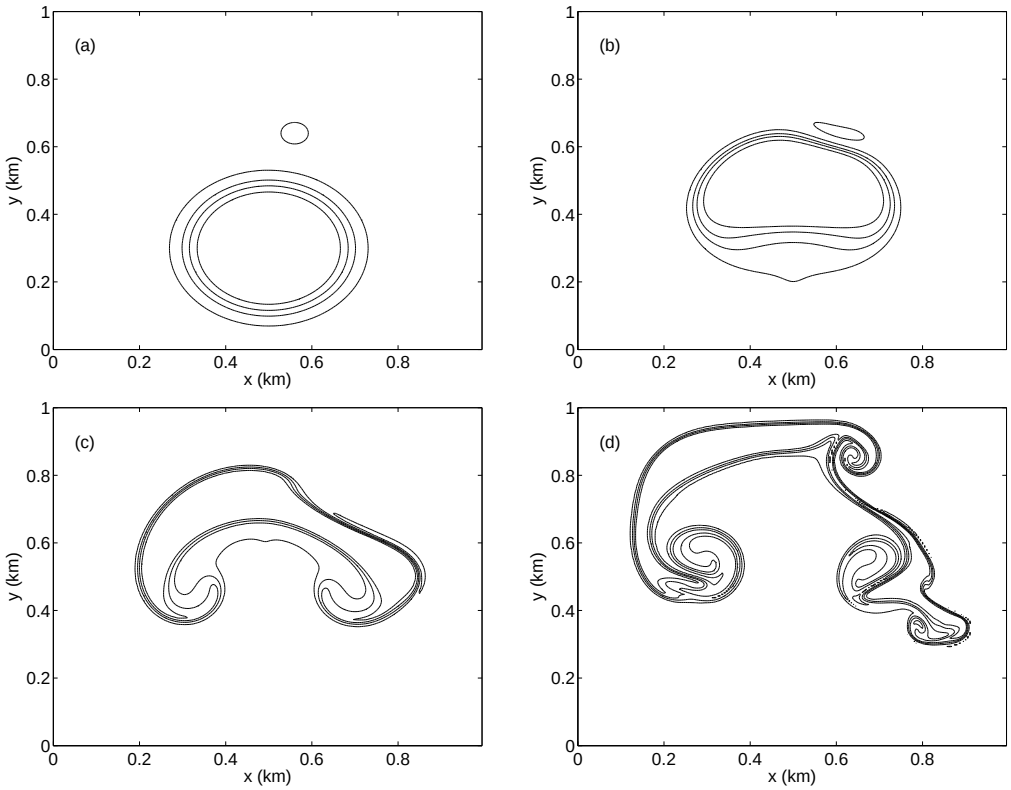

Figure 5. Potential temperature perturbations at $t = 0, 4, 7$, and 10 min for a run with a large warm bubble and a small cold bubble as initial conditions (panel (a)) for mesh-size $\Delta x = \Delta z = 5$ m and time-step $\Delta t = 2.5$ s. Contour lines are drawn at potential temperature perturbations of -0.1^o, 0.0375^o, 0.175^o, 0.3125^o, and 0.45^o C

Fig. 9 from Robert (1993). Our numerical implementation of the regularized SVSL method is identical to that of the density current experiment. The time-step is $\Delta t = 2.5$ s and corresponds to a vertical and horizontal smoothing length of $l_x \approx l_z \approx 434$ m. The numerical results can be found in Fig. 5 and agree very well with those displayed under Fig. 9 of Robert (1993).

(*e*) *Gravity wave generator*

This test is taken from Durran (1998). It is based on the following simplified equations:

$$\frac{Du'}{Dt} + \frac{\partial P}{\partial x} = -\frac{\partial \Psi}{\partial z}, \tag{95}$$

$$\frac{Dw}{Dt} + \frac{\partial P}{\partial z} - b = \frac{\partial \Psi}{\partial x}, \tag{96}$$

$$\frac{DP}{Dt} + \bar{c}_s^2 \left(\frac{\partial u'}{\partial x} + \frac{\partial w}{\partial z} \right) = 0, \tag{97}$$

$$\frac{Db}{Dt} + \bar{\mathcal{N}}^2 w = 0, \tag{98}$$

with advection operator

$$\frac{D(\cdot)}{Dt} = (\cdot)_t + (U + u')\,(\cdot)_x + w\,(\cdot)_z, \tag{99}$$

where $U(z)$ is a constant mean horizontal wind, $\Psi(x, z, t)$ is a given forcing term (see Durran (1998) page 362 for the explicit expression), $\bar{\mathcal{N}} = 0.01$ s^{-1}, and $\bar{c}_s = 350$ m s^{-1}. The regularized equations are given by

$$\frac{Du'}{Dt} + \frac{\partial \tilde{P}}{\partial x} = -\frac{\partial \Psi}{\partial z}, \tag{100}$$

$$\left(1 + \alpha^2 \bar{\mathcal{N}}^2\right) \frac{Dw}{Dt} + \frac{\partial \tilde{P}}{\partial z} - b = \frac{\partial \Psi}{\partial x}, \tag{101}$$

$$\frac{DP}{Dt} + \bar{c}_s^2 \left(\frac{\partial u'}{\partial x} + \frac{\partial w}{\partial z}\right) = 0, \tag{102}$$

$$\frac{Db}{Dt} + \bar{\mathcal{N}}^2 w = 0, \tag{103}$$

where

$$\left(1 + \alpha^2 \bar{c}_s^2 \left[\frac{\partial^2}{\partial x^2} + \frac{1}{1 + \alpha^2 \bar{\mathcal{N}}^2} \frac{\partial^2}{\partial z^2}\right]\right) \tilde{P} = P + \alpha^2 \bar{c}_s^2 \left(2 \frac{dU}{dz} \frac{\partial w}{\partial x} - \frac{\partial b}{\partial z}\right) \tag{104}$$

("nonlinear" regularization). Two test cases with constant mean wind $U = 10$ m s^{-1} and with $U(z)$ linearly increasing from 5 m s^{-1} to 15 m s^{-1}, respectively, have been implemented using the SLSV method with a step-size of $\Delta t = 12.5$ s ($l_x \approx l_z \approx 2200$ m) and mesh-sizes $\Delta x = 250$ m, $\Delta z = 50$ m. The resulting pressure fields $\tilde{P}$ at time $t = 8000$ s and $t = 3000$ s, respectively, can be found in Fig. 6. The agreement with the reference solutions, as provided by Durran (1998), is excellent and demonstrates that the regularization procedure also works for forced systems and under a strong horizontal shear flow. We stress that no divergence-damper or any other form of artificial viscosity has been applied (except for the numerical viscosity introduced by the semi-Lagrangian advection scheme).

8. Conclusions

We have presented a promising alternative to the popular SISL methodology. The new method is based on a regularized formulation of the vertical slice Euler equations, which is derived from a simple SI discretization. The temporal discretization of the regularized equations is achieved by a SL implementation of the Störmer-Verlet (SLSV) method (Reich, 2006).

The proposed SLSV method is a second-order, centred-in-time, 2-TL method and requires the solution of a single Helmholtz problem per time-step. In that regard the method is similar to 2-TL implementations of the SISL method (Temperton & Staniforth, 1987; McDonald & Bates, 1987). Note, however, that no velocity extrapolation from previous time-steps is required for the SL part of the algorithm. Since the SLSV is naturally centred-in-time there is also no need for an iterative centred-implicit implementation, as discussed by Bénard (2003), for 2-TL non-extrapolating SISL schemes. All numerical experiments were conducted without additional viscous filtering. Finally, as already pointed out in §5, the SLSV scheme can easily be combined with a mass conserving SL advection

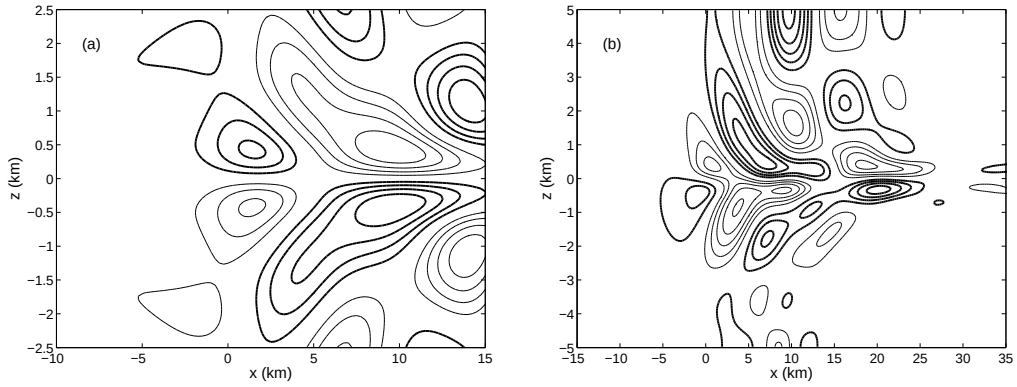

Figure 6. (a) Contours of P at intervals of 0.25 m^2 s^{-2} for constant mean advection with $U = 10$ m s^{-1}. (b) Contours of P at intervals of 0.25 m^2 s^{-2} for mean wind U linearly increasing from 5 m s^{-1} to 15 m s^{-1}. No zero contour line is shown in both cases and positive contour lines are drawn as thick lines. Only a central portion of the computational domain is shown.

scheme. See Cotter et al. (2007) for such an implementation in the context of the shallow-water equations.

Numerical results presented here and by Staniforth et al. (2007); Reich (2006); Reich et al. (2007) indicate the exciting possibility to build the SLSV method up to a fully three-dimensional fluid solver. The next steps towards this "goal" are the inclusion of orography and the treatment of vertical model equations on an f-plane along the lines of (Reich et al., 2007; Staniforth & Wood, 2007)

Acknowledgements

We would like to thank Mark Dubal and Nigel Wood for numerous discussions on the subject of this paper. We would also like to thank the two referees for valuable comments and suggestions on how to improve the paper.

References

Bénard, P. 2003 , Stability of semi-implicit and iterative centred-implicit time discretizations for various equation systems used in NWP, *Mon. Weath. Rev.* **131**, 2479–2491.

Browning, G. & Kreiss, H.-O. 1986 , Scaling and computation of smooth atmospheric motion, *Tellus* **38A**, 295–313.

Cotter, C., Frank, J. & Reich, S. 2007 , The remapped particle-mesh semi-lagrangian advection scheme, *Q.J.R. Meteorolog. Soc.* **133**, 251–260.

Davies, T., Cullen, M., Malcolm, A., Mawson, M., Staniforth, A., White, A. & Wood, N. 2005 , A new dynamical core for the Met Office's global and regional modelling of the atmosphere, *Q.J.R. Meteorolog. Soc.* **608**, 1759–1782.

Dubal, M., Staniforth, A., Wood, N. & Reich, S. 2006 , Analysis of a regularized, time-staggered discretization applied to a vertical slice model, *Atm. Sci. Lett.* **7**, 86–92.

Durran, D. 1998 , Numerical methods for wave equations in geophysical fluid dynamics, Springer-Verlag, Berlin Heidelberg.

Durran, D. R. 1989 , Improving the anelastic approximation, *J. Atmos. Sci.* **46**, 1453–1461.

Frank, J., Reich, S., Staniforth, A., White, A. & Wood, N. 2005 , Analysis of a regularized, time staggered discretization and its link to the semi-implicit method, *Atm. Sci. Lett.* **6**, 97–104.

Hinkelmann, K. 1951 , Der Mechanismus des meteorologischen Lärms, *Tellus* **3**, 285–296.

Kwizak, M. & Robert, A. 1971 , A semi-implicit scheme for grid point atmospheric models of the primitive equations, *Mon. Wea. Rev.* **99**, 32–36.

Leimkuhler, B. & Reich, S. 2005 , Simulating Hamiltonian Dynamics, Cambridge University Press, Cambridge.

Lynch, P. 1989 , The slow equations, *Q. J. R. Meteorolog. Soc.* **115**, 201–219.

Marchuk, G. 1974 , Numerical methods in weather prediction, Academic Press, New York.

McDonald, A. & Bates, J. R. 1987 , Improving the estimate of the departure point in a two-time level semi-Lagrangian and semi-implicit scheme, *Mon. Wea. Rev.* **115**, 737–739.

Reich, S. 2006 , Linearly implicit time stepping methods for numerical weather prediction, *BIT* **46**, 607–616.

Reich, S., Wood, N. & Staniforth, A. 2007 , Semi-implicit methods, nonlinear balance, and regularized equations, *Atm. Sci. Lett.* **8**, 1–6.

Robert, A. 1969 , The integration of a spectral model of the atmosphere by the implicit method, *in* 'Proc. WMO-IUGG Symp. on NWP', Vol. 7, Japan Meteorology Agency, Tokyo, pp. 19–24.

Robert, A. 1982 , A semi-Lagrangian and semi-implicit numerical integration scheme for the primitive meteorological equations, *Japan Meteor. Soc.* **60**, 319–325.

Robert, A. 1993 , Bubble convection experiments with a semi-implicit formulation of the Euler equations, *J. Atmos. Sci.* **50**, 1865–1873.

Robert, A., Henderson, J. & Turnbull, C. 1972 , An implicit time integration scheme for baroclinic models of the atmosphere, *Mon. Wea. Rev.* **100**, 329–335.

Skamarock, W. & Klemp, J. 1994 , Efficiency and accuracy of the Klemp-Wilhelmson time-splitting technique, *Mon. Wea. Rev.* **122**, 2623–2630.

Smolarkiewicz, P. & Pudykiewicz, J. 1992 , A class of semi-Lagrangian approximations for fluids, *J. Atmos. Sci.* pp. 2082–2096.

Staniforth, A. & Coté, J. 1991 , Semi-Lagrangian integration schemes for atmospheric models – A review, *Mon. Weather Rev.* **119**, 2206–2223.

Staniforth, A. & Wood, N. 2007 , Analysis of the response to orographic forcing of a TSSL discretization of the rotating SWEs, *Q.J.R. Meteorolog. Soc.* **132**, 3117–3126.

Staniforth, A., Wood, N. & Reich, S. 2007 , A time-staggered semi-Lagrangian discretization of the rotating shallow-water equations, *Q.J.R. Meteorolog. Soc.* **132**, 3107–3116.

Straka, J., Wilhelmson, R., Anderson, J. & Droegemeier, K. 1993 , Numerical solutions of a nonlinear density current - A benchmark solution and comparisons, *Int. J. Numer. Meth. in Fluids* **17**, 1–22.

Tanguay, M., Robert, A. & Laprise, R. 1990 , A semi-implicit semi-Lagrangian fully compressible regional forecast model, *Mon. Wea. Rev.* **118**, 1970–1980.

Temperton, C. & Staniforth, A. 1987 , An efficient two-time-level semi-Lagrangian semi-implicit integration scheme, *Q. J. R. Meteorol. Soc.* **113**, 1025–1039.

Wood, N., Staniforth, A. & Reich, S. 2006 , An improved regularization for time-staggered discretization and its link to the semi-implicit method, *Atm. Sci. Lett.* **7**, 21–25.

Appendix

In this appendix, we discuss a number of simplifications to the regularization (33). In part ((*d*), we also state a regularized formulation in terms of pressure, p.

(*a*) *Simplification: Pseudo-incompressibility*

Given some hydrostatic reference state, characterized by $\bar{\pi}(z)$, $\bar{\theta}(z)$, $\bar{\rho}(z)$, and $\bar{c}_s(z)$, we define

$$\mathcal{R}_\pi^R \equiv \frac{\bar{c}_s^2}{c_p \bar{\rho}\bar{\theta}^2}\left[\frac{\partial}{\partial x}\left(\bar{\rho}\bar{\theta}\mathcal{R}_u\right) + \frac{\partial}{\partial z}\left(\bar{\rho}\bar{\theta}\mathcal{R}_w\right)\right], \tag{105}$$

as well as

$$\mathcal{H}^R f \equiv f - \frac{\alpha^2 \bar{c}_s^2}{\bar{\rho}\bar{\theta}^2}\left[\frac{\partial}{\partial x}\left\{\bar{\rho}\bar{\theta}\theta\frac{\partial f}{\partial x}\right\} + \frac{\partial}{\partial z}\left\{\frac{\bar{\rho}\bar{\theta}\theta}{1+\alpha^2\mathcal{N}^2}\frac{\partial f}{\partial z}\right\}\right], \tag{106}$$

and replace (33) by

$$\mathcal{H}^R(\tilde{\pi} - \pi) = \alpha^2 \mathcal{R}_\pi^R. \tag{107}$$

We note that $\tilde{\pi} = \pi$, if

$$0 = c_p \bar{\rho}\bar{\theta}^2 \mathcal{R}_\pi^R = -\bar{c}_s^2 \frac{\partial}{\partial t}\left\{\frac{\partial}{\partial x}\left(\bar{\theta}\bar{\rho}u\right) + \frac{\partial}{\partial z}\left(\bar{\theta}\bar{\rho}w\right)\right\}, \tag{108}$$

and (108) follows from the pseudo-incompressibility approximation (Durran, 1989)

$$\frac{\partial}{\partial x}\left(\bar{\theta}\bar{\rho}u\right)+\frac{\partial}{\partial z}\left(\bar{\theta}\bar{\rho}w\right)=0. \tag{109}$$

The system (107) is equivalent to

$$\mathcal{H}^R\tilde{\pi}=\pi+\frac{\alpha^2c_s^2}{c_p\bar{\rho}\bar{\theta}^2}\left[\frac{\partial}{\partial x}\left\{\bar{\rho}\bar{\theta}\mathcal{A}(u)\right\}+\frac{\partial}{\partial z}\left\{\bar{\rho}\bar{\theta}\left(\mathcal{A}(w)+\frac{g}{1+\alpha^2\mathcal{N}^2}\right)\right\}\right]. \tag{110}$$

Note that the results of this and the following section are also valid for a general reference state of the form $\bar{\pi}(x,z)$, $\bar{\theta}(x,z)$, etc.

(*b*) *Simplification: Constant coefficient elliptic operator*

We make the same assumption as in subsection (*a*). But we apply a further simplification that leads to a constant coefficient elliptic operator $\mathcal{H}^F$. Specifically, we define

$$\mathcal{R}_\pi^F\equiv\frac{\bar{c}_s^2}{c_p\bar{\rho}\bar{\theta}^2}\left[\frac{\partial}{\partial x}\left(\bar{\rho}\bar{\theta}\mathcal{R}_u^F\right)+\frac{\partial}{\partial z}\left(\bar{\rho}\bar{\theta}\mathcal{R}_w^F\right)\right], \tag{111}$$

with

$$\mathcal{R}_u^F\equiv\frac{\bar{\theta}}{\theta}\mathcal{R}_u=\frac{\bar{\theta}}{\theta}\mathcal{A}(u)+c_p\bar{\theta}\frac{\partial\pi}{\partial x} \tag{112}$$

and

$$\mathcal{R}_w^F\equiv\frac{\bar{\theta}}{\theta}\mathcal{R}_w=\frac{\bar{\theta}}{\theta}\mathcal{A}(w)+\frac{1}{1+\alpha^2\bar{\mathcal{N}}^2}\left[c_p\bar{\theta}\frac{\partial\pi}{\partial z}+g\frac{\bar{\theta}}{\theta}\right], \tag{113}$$

as well as a constant coefficient operator, $\mathcal{H}^F$, by

$$\mathcal{H}^Ff\equiv f-\frac{\alpha^2\bar{c}_s^2}{\bar{\rho}\bar{\theta}^2}\left[\frac{\partial}{\partial x}\left\{\bar{\rho}\bar{\theta}^2\frac{\partial f}{\partial x}\right\}+\frac{\partial}{\partial z}\left\{\frac{\bar{\rho}\bar{\theta}^2}{1+\alpha^2\bar{\mathcal{N}}^2}\frac{\partial f}{\partial z}\right\}\right], \tag{114}$$

and replace (33) by

$$\mathcal{H}^F(\tilde{\pi}-\pi)=\alpha^2\mathcal{R}_\pi^F. \tag{115}$$

We note that $\tilde{\pi}=\pi$, if

$$0=c_p\bar{\rho}\bar{\theta}^2\mathcal{R}_\pi^F=-\bar{c}_s^2\left\{\frac{\partial}{\partial x}\left(\bar{\theta}\bar{\rho}\frac{\bar{\theta}}{\theta}\frac{\partial u}{\partial t}\right)+\frac{\partial}{\partial z}\left(\bar{\theta}\bar{\rho}\frac{\bar{\theta}}{\theta}\frac{\partial w}{\partial t}\right)\right\}. \tag{116}$$

It appears that (115) makes sense under the assumption that

$$\frac{\bar{\theta}}{\theta}\approx1,\quad \frac{\partial}{\partial x}\left(\frac{\bar{\theta}}{\theta}\right)\approx0,\quad \frac{\partial}{\partial z}\left(\frac{\bar{\theta}}{\theta}\right)\approx0,\quad \frac{\partial}{\partial t}\left(\frac{\bar{\theta}}{\theta}\right)\approx0 \tag{117}$$

i.e.,

$$\frac{\partial}{\partial x}\left(\frac{\bar{\theta}}{\theta}\bar{\theta}\bar{\rho}\frac{\partial u}{\partial t}\right)+\frac{\partial}{\partial z}\left(\frac{\bar{\theta}}{\theta}\bar{\theta}\bar{\rho}\frac{\partial w}{\partial t}\right)\approx\frac{\partial}{\partial t}\left[\frac{\partial}{\partial x}\left(\bar{\rho}\bar{\theta}u\right)+\frac{\partial}{\partial z}\left(\bar{\rho}\bar{\theta}w\right)\right]. \tag{118}$$

The system (115) is equivalent to

$$\mathcal{H}^F\tilde{\pi}=\pi+\frac{\alpha^2c_s^2}{c_p\bar{\rho}\bar{\theta}^2}\left[\frac{\partial}{\partial x}\left\{\frac{\bar{\rho}\bar{\theta}^2}{\theta}\mathcal{A}(u)\right\}+\frac{\partial}{\partial z}\left\{\frac{\bar{\rho}\bar{\theta}^2}{\theta}\left(\mathcal{A}(w)+\frac{g}{1+\alpha^2\bar{\mathcal{N}}^2}\right)\right\}\right]. \tag{119}$$

Finally, using (117) for the advection terms on the RHS of (119), we obtain (41).

(c) *Simplification: Incompressibility*

We can push things even further and may (under appropriate conditions) assume that

$$\frac{\mathrm{d}\bar{\pi}}{\mathrm{d}z} = 0, \qquad \frac{\mathrm{d}\bar{\theta}}{\mathrm{d}z} = 0, \qquad \bar{\mathcal{N}} = const., \qquad \bar{c}_s = const. \tag{120}$$

as well as (117). We can then simplify (115) by defining

$$\mathcal{R}_\pi^C \equiv \frac{\bar{c}_s^2}{c_p\bar{\theta}}\frac{\partial}{\partial x}\left(\mathcal{R}_u^F\right) + \frac{\bar{c}_s^2}{c_p\bar{\theta}}\frac{\partial}{\partial z}\left(\mathcal{R}_w^F\right) \tag{121}$$

as well as

$$\mathcal{H}^C f \equiv f - \alpha^2\left[\bar{c}_s^2\frac{\partial^2 f}{\partial x^2} + \frac{\bar{c}_s^2}{1+\alpha^2\bar{\mathcal{N}}^2}\frac{\partial^2 f}{\partial z^2}\right], \tag{122}$$

and replace (115) by

$$\mathcal{H}^C(\tilde{\pi} - \pi) = \alpha^2\mathcal{R}_\pi^C. \tag{123}$$

We note that $\tilde{\pi} = \pi$ is now equivalent to

$$0 = c_p\bar{\theta}^2\bar{\rho}\mathcal{R}_\pi^C \approx -\bar{c}_s^2\bar{\rho}\bar{\theta}\frac{\partial}{\partial t}\left(\frac{\partial u}{\partial x} + \frac{\partial w}{\partial z}\right). \tag{124}$$

Using (117) for the advection terms on the RHS of (123), the system (123) is further simplified to (44).

(d) *Regularized formulation in terms of pressure*

Often it is more convenient to formulate the fluid equations of motion in terms of pressure, p, instead of the Exner function, π. We state the associated regularized formulation. Specifically, we replace (28)-(31) by

$$\frac{\partial u}{\partial t} = -\mathcal{A}(u) - \frac{1}{\rho}\frac{\partial\tilde{p}}{\partial x}, \tag{125}$$

$$\frac{\partial w}{\partial t} = -\mathcal{A}(w) - \frac{1}{1+\alpha^2\mathcal{N}^2}\left[\frac{1}{\rho}\frac{\partial\tilde{p}}{\partial z} + g\right], \tag{126}$$

$$\frac{\partial p}{\partial t} = -\frac{c_s^2}{\theta}\left[\frac{\partial}{\partial x}\left\{\rho\theta u\right\} + \frac{\partial}{\partial z}\left\{\rho\theta w\right\}\right], \tag{127}$$

$$\frac{\partial\theta}{\partial t} = -\mathcal{A}(\theta), \tag{128}$$

where $\mathcal{N}$ is defined as before. The regularized pressure, $\tilde{p}$, is determined by an elliptic problem of the general form

$$\mathcal{H}^P\left(\tilde{p} - p\right) = \alpha^2\mathcal{R}_p. \tag{129}$$

The elliptic operator $\mathcal{H}^P$ and the RHS $\alpha^2\mathcal{R}_p$ are defined by

$$\mathcal{R}_p \equiv \frac{c_s^2}{\theta}\left[\frac{\partial}{\partial x}\left(\rho\theta\mathcal{R}_u\right) + \frac{\partial}{\partial z}\left(\rho\theta\mathcal{R}_w\right)\right], \tag{130}$$

with

$$\mathcal{R}_u = \mathcal{A}(u) + \frac{1}{\rho}\frac{\partial p}{\partial x}, \qquad \mathcal{R}_w = \mathcal{A}(w) + \frac{1}{1+\alpha^2\mathcal{N}^2}\left[\frac{1}{\rho}\frac{\partial p}{\partial z} + g\right], \tag{131}$$

and

$$\mathcal{H}^P f \equiv f - \frac{\alpha^2 c_s^2}{\theta}\left[\frac{\partial}{\partial x}\left\{\theta\frac{\partial f}{\partial x}\right\} + \frac{\partial}{\partial z}\left\{\frac{\theta}{1+\alpha^2\mathcal{N}^2}\frac{\partial f}{\partial z}\right\}\right], \tag{132}$$

respectively. The parameter α is determined as for the regularized formulation in terms of the Exner function π.

The constant coeffient formulation, corresponding to (115), is given by

$$\mathcal{H}^{FP}(\tilde{p}-p) = \mathcal{R}_p^F \tag{133}$$

with

$$\mathcal{R}_p^F \equiv \frac{\bar{c}_s^2}{\bar{\theta}}\left[\frac{\partial}{\partial x}\left(\rho\bar{\theta}\mathcal{R}_u\right) + \frac{\partial}{\partial z}\left(\rho\bar{\theta}\mathcal{R}_w\right)\right] \tag{134}$$

and

$$\mathcal{H}^{FP} f \equiv f - \frac{\alpha^2 \bar{c}_s^2}{\bar{\theta}}\left[\frac{\partial}{\partial x}\left\{\bar{\theta}\frac{\partial f}{\partial x}\right\} + \frac{\partial}{\partial z}\left\{\frac{\bar{\theta}}{1+\alpha^2\bar{\mathcal{N}}^2}\frac{\partial f}{\partial z}\right\}\right]. \tag{135}$$